CANCER IMMUNOLOGY

Engineered skin bacteria induce antitumor T cell responses against melanoma

Y. Erin Chen[1,2,3,4], Djenet Bousbaine[1,2,3], Alessandra Veinbachs[1,2,3], Katayoon Atabakhsh[1,2,3], Alex Dimas[1,2,3], Victor K. Yu[1,2,3], Aishan Zhao[1,2,3], Nora J. Enright[1,2,3], Kazuki Nagashima[1,2,3], Yasmine Belkaid[5,6], Michael A. Fischbach[1,2,3,7]*

Certain bacterial colonists induce a highly specific T cell response. A hallmark of this encounter is that adaptive immunity develops preemptively, in the absence of an infection. However, the functional properties of colonist-induced T cells are not well defined, limiting our ability to understand anticommensal immunity and harness it therapeutically. We addressed both challenges by engineering the skin bacterium *Staphylococcus epidermidis* to express tumor antigens anchored to secreted or cell-surface proteins. Upon colonization, engineered *S. epidermidis* elicits tumor-specific T cells that circulate, infiltrate local and metastatic lesions, and exert cytotoxic activity. Thus, the immune response to a skin colonist can promote cellular immunity at a distal site and can be redirected against a target of therapeutic interest by expressing a target-derived antigen in a commensal.

Certain members of the commensal microbiota elicit a potent T cell response upon colonization (*1*–*10*). This immune program has three defining features. First, the subtype of T cell elicited is determined by the bacterial colonist and its tissue context. For example, the gut commensal segmented filamentous bacterium induces T helper 17 (T_H17) cells (*1*), specific *Clostridium* species induce regulatory T cells (*11*), and certain strains of the skin colonist *Staphylococcus epidermidis* induce $CD8^+$ T cells (*2*). Second, colonist-induced T cells express a T cell receptor (TCR) specific for the bacterial inducer (*1*, *8*, *9*, *12*). This is a degree of specificity normally associated with an immune response to an infecting pathogen. Third, this process takes place across an intact, uninflamed epithelial barrier (*1*–*3*). Thus, physiologic colonization leads to adaptive immunity in the absence of an infection.

This work sought to answer two fundamental questions, one basic and one applied. First, we sought to understand the host's "goal" in responding to colonists by probing the functional properties of colonist-induced T cells. The $CD8^+$ T cells elicited by *S. epidermidis* are known to promote skin homeostasis and accelerate wound closure (*12*, *13*), which are unusual functions for a $CD8^+$ T cell. Are these colonist-induced immune cells capable of carrying out core functions of cellular immunity (migration and antigen-specific cytotoxicity) that are important for preventing sepsis and opportunistic infections?

Second, antigen-specific immune responses are of keen interest to researchers in oncology (*14*), infectious disease (*15*, *16*), and autoimmunity (*17*). Commensals induce antigen-specific T cells simply by colonizing, a process that is durable, safe, and avoids the undesirable side effects commonly associated with immune stimulation (*3*). Can anticommensal immunity, particularly its antigen specificity, be harnessed therapeutically by redirecting it against a target of interest?

We reasoned that both questions could be addressed by the same approach (Fig. 1A). By expressing tumor antigens in *S. epidermidis*, we could elicit T cells that were licensed by the commensal immune program but specific for a tumor. In so doing, we could probe whether these T cells were capable of leaving the colonized tissue, infiltrating a tumor, and engaging in cytotoxic activity.

Here, we show that strains of *S. epidermidis* engineered to express model antigens and tumor-derived neoantigens elicit tumor-specific $CD4^+$ and $CD8^+$ T cells upon colonization. These immune cells migrate to distal skin sites and the lungs and exhibit potent antitumor activity. *S. epidermidis* must be alive to elicit a response, suggesting that this program requires active colonization. Colonist-induced T cells synergize potently with immune checkpoint blockade. Aggressive B16-F10 melanomas are often rejected even when treatment is initiated after they are established. Thus, a commensal-directed immune program can function outside of tissue homeostasis, and engineered colonists are a simple but powerful means of generating antigen-specific T cells against a target of interest.

Engineering antigen expression into *S. epidermidis*

We chose to focus on *S. epidermidis* NIHLM087, an isolate from healthy human skin that elicits antigen-specific $CD4^+$ and $CD8^+$ T cells in mice and nonhuman primates (*2*, *3*, *12*). It does so in the context of physiologic skin colonization. There is no infection, the skin barrier is not breached, and there are no inflammatory processes (*2*, *3*, *13*, *18*).

Even though *S. epidermidis* is a ubiquitous human colonist, genetic manipulation of primary human isolates such as NIHLM087 is challenging because *S. epidermidis* has stringent restriction systems and phage-transduction susceptibility that differ substantially among strains (*19*–*22*), and as with other Gram-positive bacteria, electroporation is an inefficient means of introducing DNA (*23*). We developed a genetic system for *S. epidermidis,* which includes a previously described method of passaging plasmids through *Escherichia coli* DC10B (Δ*dcm*) and also incorporates heat shock and growth in hyperosmolar sorbitol (*24*) (Fig. 1B). This system enabled us to construct mutations in 13 of the 17 *S. epidermidis* strains that we tested, including primary human isolates from diverse phylogenetic groups (Fig. 1C).

We next sought to engineer *S. epidermidis* NIHLM087 (hereafter, *S. epidermidis*) to express non-native antigens. Notably, the process that determines which *S. epidermidis* antigens are selected for presentation from among thousands of distinct proteins in the bacterial cell has not been studied, so it was unclear whether a non-native peptide could compete against native *S. epidermidis* antigens for $CD8^+$ T cell recognition.

Our strategy accounted for this element of uncertainty (Fig. 1D). We began with ovalbumin (OVA) as a model antigen because it harbors well-characterized antigenic peptides that are recognized by OVA-specific $CD8^+$ or $CD4^+$ T cells (OT-I or OT-II, respectively). We were unsure whether a non-native antigen could be expressed in an undomesticated human isolate at a high enough level to be presented on the surface of an antigen-presenting cell, or whether the subcellular localization of the antigen in *S. epidermidis* would affect its processing and presentation. We therefore generated three sets of strains in which the nature of the antigen and its localization were varied. One strain for cytoplasmic expression consisted solely of full-length OVA (cOVA). Another three strains were designed for antigen displayed on the cell wall in which OVA, OT-I, or OT-II was spliced between the N-terminal sortase signal peptide and a C-terminal cell wall–spanning region from *S. aureus* protein A (*25*). This approach yielded *S. epi*-wOVA, *S. epi*-wOT-I, and *S. epi*-wOT-II, respectively ("w" denotes "wall-attached."). Three more strains were generated for antigen secretion,

[1]Department of Bioengineering, Stanford University, Stanford, CA 94305, USA. [2]Department of Microbiology and Immunology, Stanford University School of Medicine, Stanford, CA 94305, USA. [3]ChEM-H Institute, Stanford University, Stanford, CA 94305, USA. [4]Dermatology Service, San Francisco Veterans Administration Health Care System, San Francisco, CA 94121, USA. [5]Metaorganism Immunity Section, Laboratory of Host Immunity and Microbiome, National Institute of Allergy and Infectious Diseases, National Institutes of Health, Bethesda, MD 20892, USA. [6]NIAID Microbiome Program, National Institute of Allergy and Infectious Diseases, Bethesda, MD 20892, USA. [7]Chan Zuckerberg Biohub, Stanford, CA 94305, USA.
*Corresponding author. Email: fischbach@fischbachgroup.org

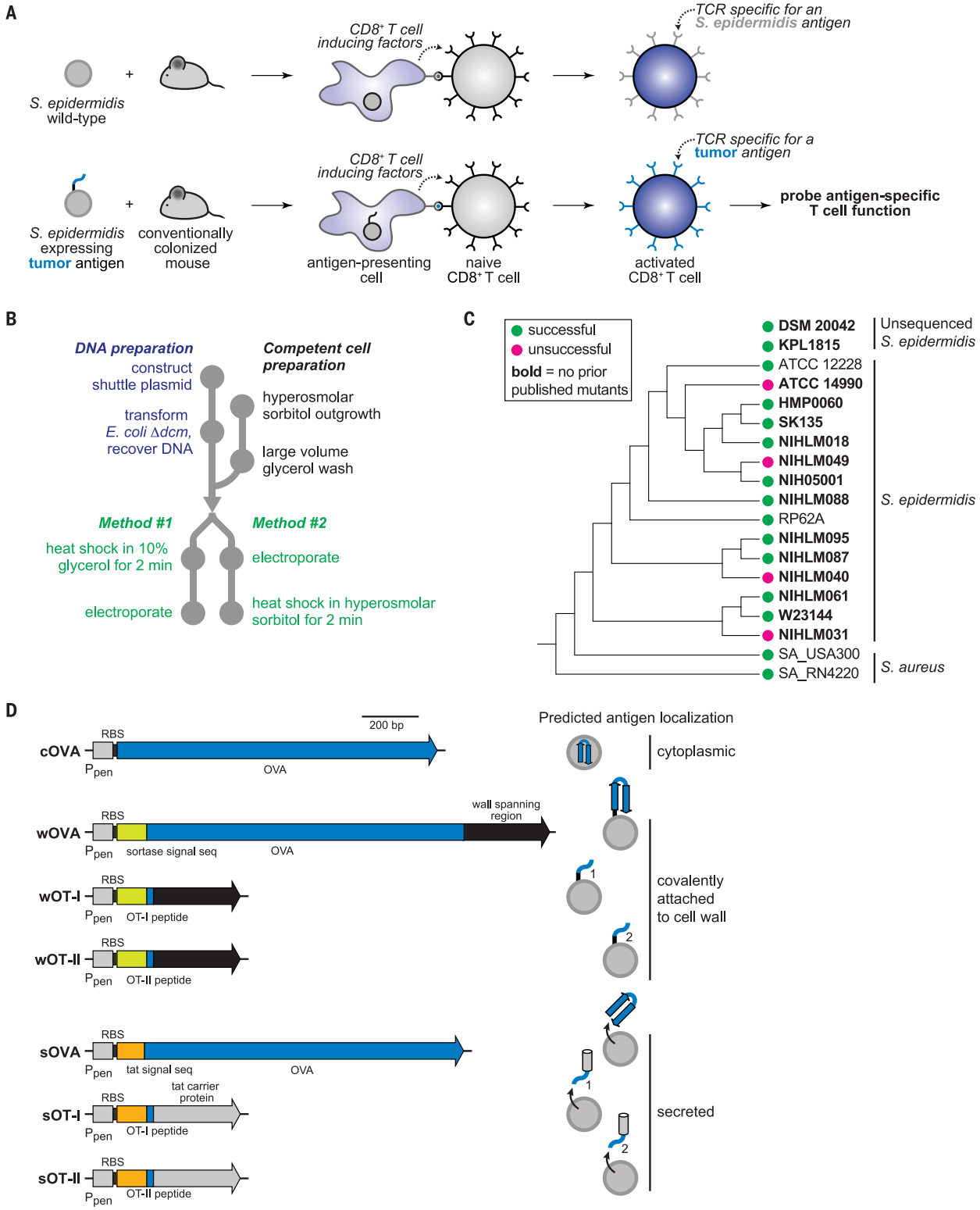

Fig. 1. Engineering *S. epidermidis* to express non-native antigens. (**A**) Experimental approach. By colonizing mice with an engineered strain of *S. epidermidis* that expresses a tumor antigen, we elicit T cells in vivo that are licensed by the commensal immune program but specific for a tumor. These T cells can then be subjected to functional assays in vivo, such as tumor killing. (**B**) Schematic of the genetic system that we developed for *S. epidermidis*. Advances include improved preparation of DNA and competent cells (materials and methods). *Staphylococcus* is subjected to heat shock before (Method #1) or after (Method #2) electroporation with the plasmid. (**C**) Phylogenetic tree of *S. epidermidis* and *S. aureus* strains. Circles indicate the strains for which our transformation method was successful (green) or unsuccessful (magenta). Strains in bold were not previously published as genetically tractable. (**D**) Design of the ovalbumin (OVA)–derived constructs expressed in *S. epidermidis* and their predicted localization. OVA is expressed either as a full-length protein (OVA), a class I major histocompatibility complex (MHC)–restricted antigenic peptide (OT-I, "1"), or a class II MHC-restricted antigenic peptide (OT-II, "2"). RBS, ribosome binding site; P_{pen}, promoter; bp, base pair.

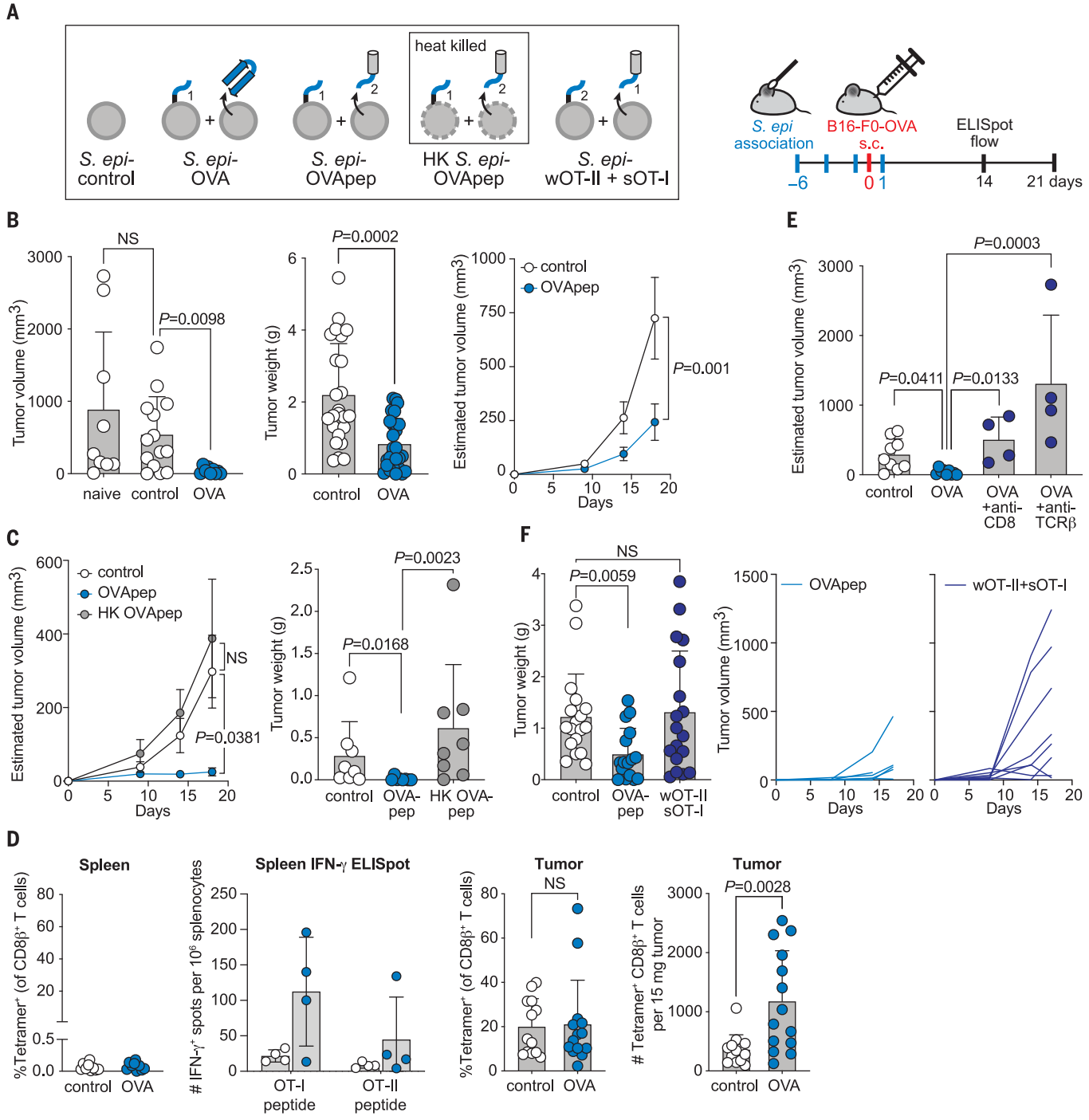

Fig. 2. Engineered *S. epidermidis* strains slow tumor progression and stimulate antigen-specific T cells in vivo. (**A**) Experimental schematic. Mice are naïve or colonized with live or heat-killed (HK; 95°C for 30 min) *S. epidermidis* strains (shown in box; OT-I, "1"; OT-II, "2") on days −6 to +1. When HK is used, mice are associated twice weekly throughout the entire experiment. On day 0, B16-F0-OVA melanoma cells are injected subcutaneously into the flank. Tissues are collected for analysis on days 14 or 21. (**B**) (Left) Day 19 blinded caliper measurements of subcutaneous B16-F0-OVA tumors (n = 5 to 10 mice per group). (Middle) Day 21 masses of dissected tumors (n = 24 to 28 mice per group). (Right) Blinded caliper measurements of tumors over time (n = 16 mice per group). (**C**) (Left) Blinded caliper measurements over time and (right) masses of subcutaneous B16-F0-OVA tumors on day 21 from mice associated with live or HK strains (gray dots). (**D**) Frequency of OT-I-specific T cells in the indicated organs as measured by H2-K^b-SIINFEKL tetramer staining or IFN-γ$^+$ ELISpot assay at day 14. Tetramer staining is gated on live CD90.2$^+$TCRβ$^+$CD8β$^+$ cells. (**E**) Endpoint caliper measurements of tumors from *S. epidermidis*–associated mice treated or not with anti-CD8α (2.43) or anti-TCRβ (H57-597) neutralizing antibodies (dark blue dots) (n = 4 to 9 mice per group). (**F**) Masses of subcutaneous B16-F0-OVA tumors on day 21 from mice colonized with *S. epidermidis* harboring control or various OVA constructs (n = 8 to 10 mice per group). For tumor burden bar graphs, nonparametric testing was used to generate P values (Mann-Whitney U test for two groups and Kruskal-Wallis H test for more than two groups). For flow cytometry data, parametric testing was used (unpaired Student's t test). For tumor-growth time courses, two-way analysis of variance (ANOVA, mixed-effects model) with multiple comparison testing was used. All experiments show unilateral tumors pooled from two [(B), left and right, (E), and (F)] or three [(B), middle] independent experiments.

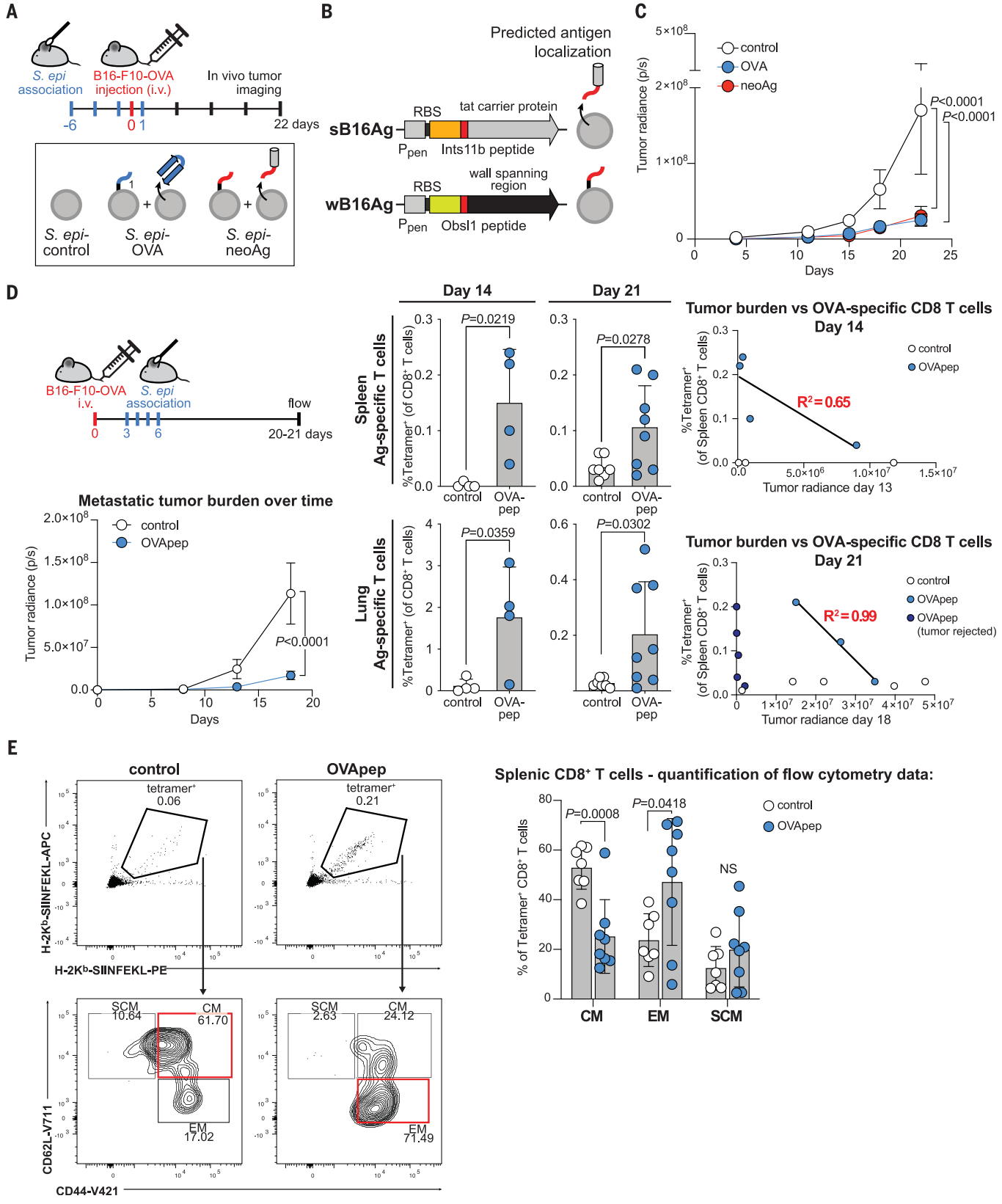

Fig. 3. Engineered *S. epidermidis* strains slow the progression of metastatic tumors. (**A**) Study design. Mice associated with *S. epidermidis* strains are injected intravenously (day 0) with B16-F10-OVA melanoma cells that constitutively express luciferase (OT-I, "1"). (**B**) Schematic of neoantigen expression constructs and their predicted subcellular localization within *S. epidermidis*. The neoantigen sequence (red box) encodes peptides centered around Obsl1(T1764M) for the wall-attached construct (wB16Ag) or Ints11(D314N) for the secreted construct (sB16Ag). (**C**) Average measurement of tumor bioluminescence over time (n = 20 mice per group, two experiments pooled). (**D**) Treatment of metastatic B16-F10-OVA melanoma with association of

S. epi-OVApep. (Left) Tumor burden over time as quantified by bioluminescence imaging. (Middle) Frequency of OT-I–specific T cells in the spleen at days 14 and 21 by H2-K^b-SIINFEKL tetramer staining. Cells are gated on live CD90.2$^+$ TCRβ$^+$ CD8β$^+$ cells. (Right) Frequency of tetramer$^+$ CD8$^+$ T cells versus tumor radiance. (**E**) Memory cell phenotypes of tetramer$^+$ CD8$^+$ T cells in the spleens of control or treated mice with metastatic melanoma. SCM, stem cell–like memory; CM, central memory; EM, effector memory. For tumor burden bar graphs, nonparametric testing was used to generate *P* values (Mann-Whitney *U* test for two groups and Kruskal-Wallis *H* test for more than two groups). For flow cytometry data, parametric testing was used (unpaired Student's *t* test). For tumor growth time courses, two-way ANOVA (mixed-effects model) with multiple comparison testing was used.

in which OT-I or OT-II was spliced into the secreted protein FepB (Tat pathway) (*26*, *27*) at the predicted signal sequence cleavage site or full-length OVA was fused to the N-terminal signal sequence (*S. epi*-sOT-I, *S. epi*-sOT-II, and *S. epi*-sOVA; "s" denotes "secreted."). We verified the production and localization of the OVA constructs by immunoblot and electron microscopy (fig. S1). Although *S. epidermidis* has no described Tat secretion system, the Tat signal peptide enabled efficient production and secretion of OVA.

Engineered strains of *S. epidermidis* stimulate antigen-specific T cells in vitro and in vivo

The engineered strains of *S. epidermidis* could stimulate antigen-specific T cells in vitro (fig. S2), so we tested whether they could prime T cells in vivo (fig. S3). Wild-type (WT) specific pathogen–free (SPF) C57BL/6 mice were topically colonized with *S. epi*-wOT-I or *S. epi*-sOT-II followed by the adoptive transfer of OT-I or OT-II cells. OT-I– or OT-II–expressing *S. epidermidis* could prime OVA-specific CD8$^+$ or CD4$^+$ T cells, respectively, without any barrier breach or skin inflammation (fig. S3A). Thus, under physiologic conditions of colonization, engineered *S. epidermidis* strains stimulate T cells specific for non-native epitopes.

S. epidermidis-OVA-induced T cells slow the progression of subcutaneous melanoma

We next sought to determine whether colonization with engineered *S. epidermidis* could elicit OVA-specific T cells from the native polyclonal repertoire, and if so, whether they would be functionally equipped to exert antitumor activity.

WT SPF C57BL/6 mice were injected subcutaneously with B16-F0-OVA, a C57BL/6-derived melanoma cell line that expresses ovalbumin. Mice were either unassociated (naïve) or gently swabbed with live *S. epidermidis* (Fig. 2A). Control mice were associated with a strain of *S. epidermidis* engineered to express an unrelated protein (*S. epi*-control). Treated mice were associated with a combination of *S. epi*-wOT-I and *S. epi*-sOVA (hereafter, "*S. epi*-OVA") or a combination of *S. epi*-wOT-I and *S. epi*-sOT-II (hereafter, "*S. epi*-OVApep") to elicit OVA-specific CD8$^+$ and CD4$^+$ T cells (fig. S3) because both T cell populations are required for optimal control of B16 melanoma (*28*). *S. epi*-OVA or *S. epi*-OVApep colonization markedly reduced tumor growth (Fig. 2B). *S. epi*-control colonization did not reduce tumor growth as compared with the absence of colonization (Fig. 2B). Thus, the antitumor effect is not due to an increased number of *S. epidermis*–specific CD8$^+$ T cells or a change in immune tone. This effect instead appears to be mediated by OVA-specific T cells because *S. epidermidis* exerts antitumor activity only when OVA is present.

Heat-killing *S. epi*-OVApep abolished the antitumor response (Fig. 2C), consistent with the observation that heat-killed *S. epi*-wOT-I failed to prime OT-I T cells in vivo (fig. S3B). Thus, the engineered bacterial colonist is not simply a source of antigen and adjuvant. Rather, bacterial viability, occupancy of specialized niches, and (potentially) prolonged antigen exposure may be required for the immune stimulatory response, even though no infection is mounted.

Next, we asked whether the antitumor effect was mediated by the OVA-specific T cells elicited by engineered *S. epidermidis*. First, compared with *S. epi*-control colonization, colonization with *S. epi*-OVApep caused increased infiltration of OVA-specific CD8$^+$ T cells into the tumor and an increase in OVA-specific interferon-γ (IFN-γ)$^+$ CD8$^+$ and CD4$^+$ T cells in the spleen (Fig. 2D and fig. S4A). The skin of tumor-bearing mice contained very limited numbers of OVA-specific CD8$^+$ T cells, which were biased toward the production of IFN-γ over interleukin-17A (fig. S4, B to D). Furthermore, there was no evidence of skin or systemic inflammation, in contrast to immunization with OVA-CFA (figs. S5 and S6). Thus, OVA-specific T cells elicited by *S. epidermidis* can migrate to and infiltrate a tumor without skin or systemic toxicity.

Second, we depleted CD8$^+$ T cells or all αβ T cells in tumor-bearing, *S. epi*-OVA–colonized mice. In both cases, the therapeutic effect of *S. epi*-OVA colonization was eliminated (Fig. 2E and fig. S4F). When mice were associated with either *S. epi*-wOT-I or *S. epi*-sOT-II rather than the combination of both, tumor weights were not significantly reduced, suggesting that OVA-specific CD4$^+$ and CD8$^+$ T cells were both required. When the subcellular localization of OT-I and OT-II in *S. epidermidis* was swapped by colonizing with *S. epi*-wOT-II plus *S. epi*-sOT-I, the antitumor effect was also lost, even though these strains are respectively capable of priming CD4$^+$ OT-II and CD8$^+$ OT-I cells (Fig. 2F and fig. S3B). Thus, the minimal requirements for antitumor efficacy are a wall-attached CD8$^+$ antigen and a CD4$^+$ antigen. Furthermore, in vivo priming of OVA-specific T cells does not completely predict their functional outcome. More broadly, our findings are consistent with a model in which *S. epidermidis*–induced T cells enter circulation, infiltrate the tumor, and are required for antitumor activity.

S. epidermidis–induced T cells are active in tissues distinct from the site of colonization

S. epi-OVA–induced T cells can limit subcutaneous tumor growth. Even though *S. epidermidis* is a skin colonist, we wondered whether *S. epidermidis*–induced T cells could traffic into other tissues. We reasoned that translocation of microbial colonists across barrier tissues can cause life-threatening sepsis, so one of the central goals of barrier immunity may be to limit systemic microbial dissemination.

To address this question, we used B16-F10, a more aggressive variant of B16, in a model of metastatic melanoma. Luciferase-expressing B16-F10-OVA cells were injected intravenously, resulting in lung metastases, which were quantified with in vivo luminescence imaging (Fig. 3A and fig. S7A). Topical colonization with *S. epi*-OVA before intravenous tumor cell injection slowed tumor progression substantially, and in some cases, promoted tumor rejection or near-rejection (Fig. 3C and fig. S7B). Thus, the antitumor effect of *S. epi*-OVA is not restricted to the skin and subcutaneous tissues.

The potency of the antitumor response induced by *S. epi*-OVA was unexpected. Even when used as monotherapy, colonist-induced T cells limited the growth of an aggressive tumor, which is notable because colonization is a mild treatment and does not induce any of the normal side effects of immune stimulation. This result is consistent with the view that *S. epidermidis* could be used as a tool for eliciting antigen-specific T cells in situ. Antigen-specific T cells generated by other methods (ex vivo engineering) are expensive (*29*), prone to exhaustion (*30*, *31*), and have had limited success in treating solid tumors (*32*). Thus, we tested whether *S. epi*–induced T cells have functional attributes that would enable them to be useful in a real-world setting, such as specificity for real-world antigens, activity against established tumors, and synergy with existing immunotherapies.

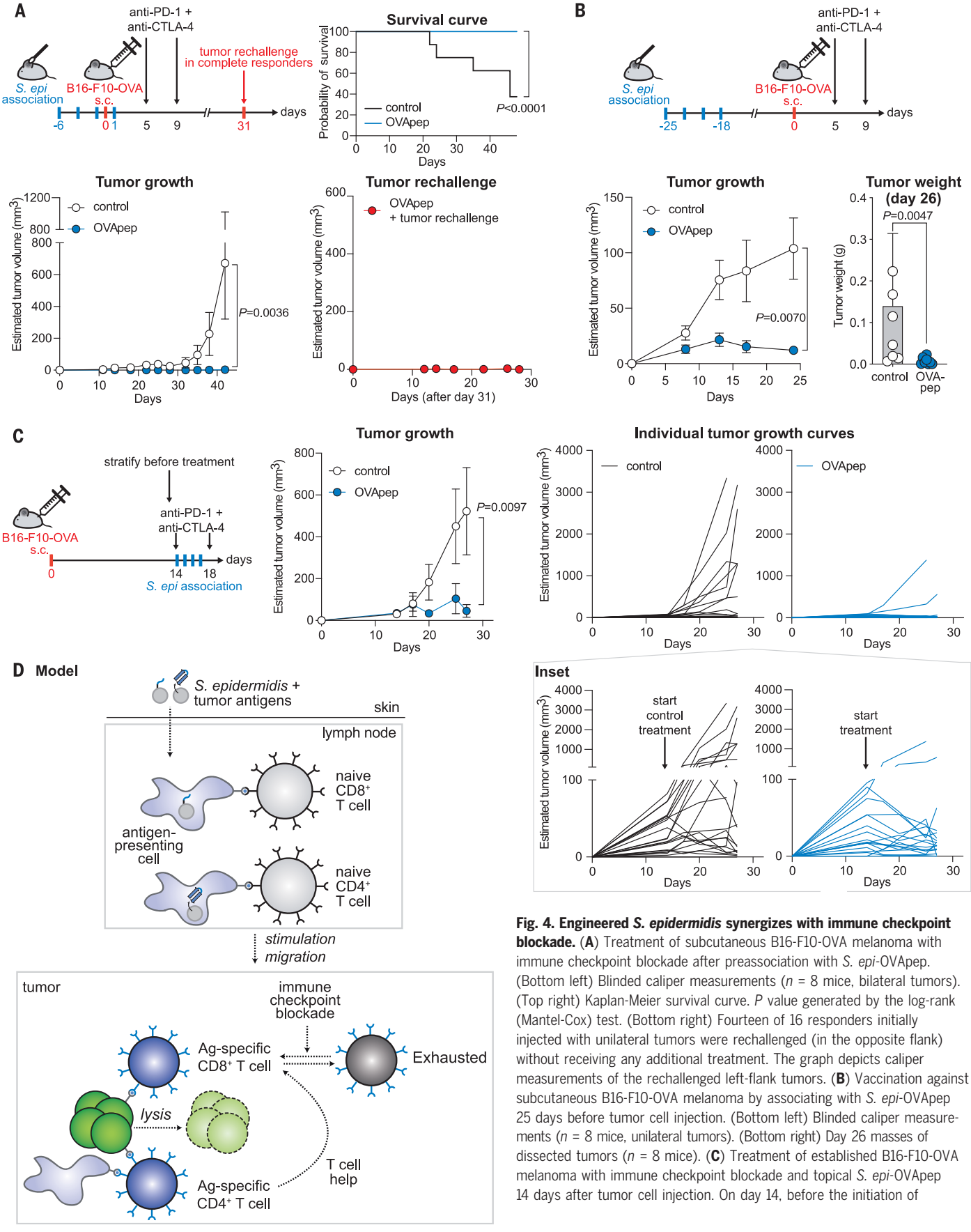

Fig. 4. Engineered *S. epidermidis* synergizes with immune checkpoint blockade. (**A**) Treatment of subcutaneous B16-F10-OVA melanoma with immune checkpoint blockade after preassociation with *S. epi*-OVApep. (Bottom left) Blinded caliper measurements (n = 8 mice, bilateral tumors). (Top right) Kaplan-Meier survival curve. P value generated by the log-rank (Mantel-Cox) test. (Bottom right) Fourteen of 16 responders initially injected with unilateral tumors were rechallenged (in the opposite flank) without receiving any additional treatment. The graph depicts caliper measurements of the rechallenged left-flank tumors. (**B**) Vaccination against subcutaneous B16-F10-OVA melanoma by associating with *S. epi*-OVApep 25 days before tumor cell injection. (Bottom left) Blinded caliper measurements (n = 8 mice, unilateral tumors). (Bottom right) Day 26 masses of dissected tumors (n = 8 mice). (**C**) Treatment of established B16-F10-OVA melanoma with immune checkpoint blockade and topical *S. epi*-OVApep 14 days after tumor cell injection. On day 14, before the initiation of

treatment, mice with no tumors or particularly large tumors (>100 mm^3) were excluded from the analysis. Blinded caliper measurements are shown (middle) averaged or (right) as growth curves of individual tumors. Inset with segmented *y* axis shows tumors initially growing and then regressing after treatment (n = 19 to 20 mice, unilateral tumors). For bar graphs, the Mann-Whitney *U* test was used to generate *P* values. For tumor growth time courses, two-way ANOVA with multiple comparison testing was used. (**D**) Model: Engineered strains of *S. epidermidis* colonize the skin and induce antigen-presenting cells to stimulate antigen-specific T cells, which traffic to the tumor and restrict tumor growth. Immune checkpoint blockade synergizes with engineered commensals. All data shown are representative of two independent experiments.

S. epidermidis producing a native neoantigen slows tumor progression

We asked whether *S. epidermidis* could elicit T cells specific for a real tumor antigen, and if so, whether their antitumor activity would be comparable to that of OVA-specific T cells. We engineered *S. epidermidis* to express two neoantigen-containing peptides (termed "*S. epi*-neoAg") naturally present in B16-F10 melanoma that were previously shown to generate $CD8^+$ and $CD4^+$ T cell responses (*33*) (Fig. 3B). Colonization with *S. epi*-neoAg before intravenous injection of B16-F10-OVA cells potently restricted metastatic tumor growth (Fig. 3, A to C, and fig. S7, A and B). A similar approach also reduced tumor progression in the TRAMP-C2 prostate carcinoma model (fig. S8) (*34*). Thus, commensal-induced T cells can be redirected against multiple host antigens and in different tumor contexts.

S. epi-OVApep colonization is effective after tumor cell injection

Next, we tested whether colonizing mice with engineered *S. epidermidis* after tumor cell injection would yield a therapeutic response. Using the intravenous B16-F10-OVA model of metastatic melanoma, we colonized with *S. epi*-OVApep starting 3 days after tumor inoculation (Fig. 3D). The reduction in tumor burden was comparable to the prophylaxis model and was accompanied by an increase in OVA-specific $CD8^+$ T cells in both the lung and spleen. The frequency of splenic OVA-specific $CD8^+$ T cells correlated well with the reduction in tumor burden in *S. epi*-OVApep–associated mice but not in control mice (Fig. 3D, right), supporting the hypothesis that *S. epi*-OVApep–induced $CD8^+$ T cells are important for metastatic tumor control.

Because control mice also had OVA-specific $CD8^+$ T cells circulating in the lung and spleen due to antigen exposure from the tumor, albeit a smaller number than in *S. epi*-OVApep–colonized mice, we asked whether the OVA-specific T cells differed functionally between control and treatment mice. We observed an unusual shift in the OVA-specific $CD8^+$ T cell pool from mostly central memory cells in control mice to effector or effector memory cells in *S. epi*-OVApep–associated mice (Fig. 3E and fig. S7D). Thus, *S. epi*-OVA–primed T cells are functionally distinct from tumor-primed T cells, even when they share the same antigen specificity. The effector phenotype of *S. epi*-OVA–primed T cells may explain their enhanced capacity to control tumors (*35*–*37*).

Engineered *S. epidermidis* synergizes with immune checkpoint blockade

The therapeutic effect of *S. epi*-OVA is likely mediated by effector and effector memory T cells that can become exhausted in the tumor environment (*38*, *39*), and a large proportion of *S. epi*-OVA–induced tumor-infiltrating lymphocytes (TILs) were positive for programmed cell death protein–1 (PD-1), a marker of exhaustion (fig. S9, A to C) (*40*). Therefore, we reasoned that adding immune checkpoint blockade would relieve the exhaustion of *S. epi*-OVA–induced TILs and augment antitumor activity.

We tested this hypothesis in the setting of subcutaneous B16-F10-OVA, which does not respond to immune checkpoint blockade alone (*41*, *42*). In contrast to *S. epi*-control colonization, *S. epi*-OVApep colonization combined with immune checkpoint blockade led to the rejection of 15 of 16 tumors (Fig. 4A). In a repeat experiment, we initially injected tumors in the right flank and 31 days later challenged the complete responders with left-flank tumors. All mice rejected the left-flank tumors, and 9 of 14 mice continued to be tumor free in the right flank 2 months after the initial tumor challenge (Fig. 4A). Furthermore, we could vaccinate mice against melanoma by associating them 25 days before tumor inoculation, by which time the effector T cell response to *S. epi*-OVApep would have contracted (Fig. 4B) (*3*). Thus, the memory T cell response elicited by earlier *S. epi*-OVApep association in combination with checkpoint blockade is sufficient to restrict tumor growth.

Next, we tested whether a combination of engineered *S. epidermidis* and checkpoint inhibition could treat established tumors. We waited either 5 or 14 days after B16-F10-OVA inoculation to colonize mice with *S. epi*-control or *S. epi*-OVApep and administer immune checkpoint blockade. The reduction in tumor burden was almost as pronounced as in the prophylaxis model, with regression of most tumors (Fig. 4C and fig. S9D). No inflammation, increase in ear thickness, or significant OVA-specific T cell infiltration of the skin was observed (fig. S4B and fig. S5, B to D). Thus, the combination of a tumor antigen-expressing commensal with checkpoint blockade yields a potent and durable antitumor response that can treat well-established tumors.

Discussion

Our approach, which uses a commensal microbe as the adjuvant and colonization as the mode of tumor antigen delivery, differs from previous strategies in important ways. In contrast to recent studies with native bacterial species from the gut microbiome, we find that the antitumor activity of *S. epidermidis* is not due to a change in the innate immune milieu or to an increase in colonist-specific $CD8^+$ T cells (*43*–*46*). Rather, it requires the tumor antigen to be present. Moreover, colonization with *S. epi*-OVA does not result in an infection, require intratumoral delivery, or generate any measurable inflammation, making it safer, simpler, and more specific than approaches that require inflammation or tissue infiltration for antitumor activity (*47*–*49*).

Our approach is more comparable to other means of generating tumor-specific T cells, such as ex vivo T cell engineering [to generate chimeric antigen receptor (CAR) T and TCR T cells] and tumor vaccines. Although much research still needs to be done, engineered *S. epidermidis* is safe and simple and yields a potent antitumor response in combination with checkpoint blockade. This is notable, given that B16-F10 melanoma is an unusually fast-growing and immunologically cold cancer. Other approaches that have yielded comparable treatment outcomes have been far more aggressive (*50*–*52*). Colonist-induced T cells appear to have different functional properties than antigen-specific T cells generated by other means. We found that *S. epi*-OVA–induced $CD8^+$ T cells were biased toward an effector memory (rather than central memory) phenotype, which may explain their potency within a tumor. In contrast to vaccination methods that are episodic, a colonist may provide continuous, durable stimuli over multiple weeks, leading to a prolonged supply of effector T cells.

The immune memory that we observed in combination with checkpoint blockade is notable, given that the plasmid was lost (fig. S10). This indicates that even a week of antigen exposure can induce a long-lasting response, even if this exposure occurs much earlier than the tumor challenge. In the future, a strain that expresses antigen stably may lead to more prolonged antigen exposure—the equivalent of a "prime" and a constant "boost"—and consequently, a more robust memory immune cell response. Furthermore, the observation of tumor

rejection in some mice in treatment mode, combined with the observation that *S. epidermidis* induces $CD8^+$ T cells in nonhuman primates (*12*), suggests this may be a credible strategy for translation.

More broadly, our results imply that it might be possible to engineer antigen expression into other commensal bacterial strains to elicit a wide range of antigen-specific immune cell responses. Understanding how to redirect each one may open the door to immunotherapies for other diseases and deepen our understanding of commensal–host interactions.

REFERENCES AND NOTES

1. Y. Yang *et al*., *Nature* **510**, 152–156 (2014).
2. S. Naik *et al*., *Science* **337**, 1115–1119 (2012).
3. S. Naik *et al*., *Nature* **520**, 104–108 (2015).
4. T. C. Scharschmidt *et al*., *Immunity* **43**, 1011–1021 (2015).
5. V. K. Ridaura *et al*., *J. Exp. Med.* **215**, 785–799 (2018).
6. H. Chung *et al*., *Cell* **149**, 1578–1593 (2012).
7. M. Xu *et al*., *Nature* **554**, 373–377 (2018).
8. E. Ansaldo *et al*., *Science* **364**, 1179–1184 (2019).
9. M. M. Wegorzewska *et al*., *Sci. Immunol.* **4**, eaau9079 (2019).
10. L. Cervantes-Barragan *et al*., *Science* **357**, 806–810 (2017).
11. K. Atarashi *et al*., *Science* **331**, 337–341 (2011).
12. J. L. Linehan *et al*., *Cell* **172**, 784–796.e18 (2018).
13. O. J. Harrison *et al*., *Science* **363**, eaat6280 (2019).
14. A. K. Palucka, L. M. Coussens, *Cell* **164**, 1233–1247 (2016).
15. N. N. Jarjour, D. Masopust, S. C. Jameson, *Immunity* **54**, 14–18 (2021).
16. T. Carvalho, F. Krammer, A. Iwasaki, *Nat. Rev. Immunol.* **21**, 245–256 (2021).
17. H. B. Streeter, D. C. Wraith, *Curr. Opin. Immunol.* **70**, 75–81 (2021).
18. S. Tamoutounour *et al*., *Proc. Natl. Acad. Sci. U.S.A.* **116**, 23643–23652 (2019).
19. J. Y. H. Lee *et al*., *Microb. Genom.* **2**, e000077 (2016).
20. I. R. Monk, I. M. Shah, M. Xu, M.-W. Tan, T. J. Foster, *mBio* **3**, e00277-11 (2012).
21. I. R. Monk, J. J. Tree, B. P. Howden, T. P. Stinear, T. J. Foster, *mBio* **6**, e00315 (2015).
22. V. Winstel, P. Kühner, H. Rohde, A. Peschel, *Nat. Protoc.* **11**, 949–959 (2016).
23. J. L. Moran, N. N. Dingari, P. A. Garcia, C. R. Buie, *Bioelectrochemistry* **123**, 261–272 (2018).
24. S. K. Costa, N. P. Donegan, A.-R. Corvaglia, P. François, A. L. Cheung, *J. Bacteriol.* **199**, e00271-17 (2017).
25. M. Hansson *et al*., *J. Bacteriol.* **174**, 4239–4245 (1992).
26. L. Biswas *et al*., *J. Bacteriol.* **191**, 5921–5929 (2009).
27. E. Turlin, M. Débarbouillé, K. Augustyniak, A.-M. Gilles, C. Wandersman, *PLOS ONE* **8**, e56529 (2013).
28. J. Kline, L. Zhang, L. Battaglia, K. S. Cohen, T. F. Gajewski, *J. Immunol.* **188**, 2630–2642 (2012).
29. C. H. June, R. S. O'Connor, O. U. Kawalekar, S. Ghassemi, M. C. Milone, *Science* **359**, 1361–1365 (2018).
30. E. W. Weber *et al*., *Science* **372**, eaba1786 (2021).
31. R. C. Lynn *et al*., *Nature* **576**, 293–300 (2019).
32. L. Lindo, L. H. Wilkinson, K. A. Hay, *Front. Immunol.* **11**, 618387 (2021).
33. S. Kreiter *et al*., *Nature* **520**, 692–696 (2015).
34. B. A. Foster, J. R. Gingrich, E. D. Kwon, C. Madias, N. M. Greenberg, *Cancer Res.* **57**, 3325–3330 (1997).
35. S. van Duikeren *et al*., *J. Immunol.* **189**, 3397–3403 (2012).
36. M. Enamorado *et al*., *Nat. Commun.* **8**, 16073 (2017).
37. T. N. Gide *et al*., *Cancer Cell* **35**, 238–255.e6 (2019).
38. F. S. Hodi *et al*., *N. Engl. J. Med.* **363**, 711–723 (2010).
39. J. R. Brahmer *et al*., *N. Engl. J. Med.* **366**, 2455–2465 (2012).
40. K. Sakuishi *et al*., *J. Exp. Med.* **207**, 2187–2194 (2010).
41. D. Zamarin *et al*., *Sci. Transl. Med.* **6**, 226ra32 (2014).
42. C. Twyman-Saint Victor *et al*., *Nature* **520**, 373–377 (2015).
43. M. Sade-Feldman *et al*., *Cell* **175**, 998–1013.e20 (2018).
44. V. Gopalakrishnan *et al*., *Science* **359**, 97–103 (2018).
45. B. Routy *et al*., *Science* **359**, 91–97 (2018).
46. T. Tanoue *et al*., *Nature* **565**, 600–605 (2019).
47. Y. Paterson, P. D. Guirnalda, L. M. Wood, *Semin. Immunol.* **22**, 183–189 (2010).
48. C.-Z. Wang, R. A. Kazmierczak, A. Eisenstark, *Int. J. Microbiol.* **2016**, 5678702 (2016).
49. D. C. Binder *et al*., *Cancer Immunol. Res.* **1**, 123–133 (2013).
50. W. W. Overwijk *et al*., *J. Exp. Med.* **198**, 569–580 (2003).
51. W. W. Overwijk, N. P. Restifo, *Curr. Protoc. Immunol.* **39**, 20.1.1–20.1.29 (2001).
52. D. C. Palmer *et al*., *Proc. Natl. Acad. Sci. U.S.A.* **105**, 8061–8066 (2008).

ACKNOWLEDGMENTS

We are indebted to members of the Fischbach Group for helpful suggestions and comments on the manuscript. We are grateful to N. Collins, E. Enamorado, T. Yamamoto, R. Tussiwand, and S. Park for helpful discussions and to H. Pimentel and J. Rajniak for guidance on statistical analyses. We are indebted to the Stanford animal facility staff for help with animal husbandry. Cell sorting and flow cytometry analyses were performed on instruments in the Stanford Shared FACS Facility with help from M. Weglarz, L. Nichols, and R. Zermeno. Electron micrographs were generated by the Washington University Center for Cellular Imaging supported by Washington University School of Medicine in St. Louis, The Children's Discovery Institute of Washington University and St. Louis Children's Hospital (CDI-CORE-2015-505 and CDI-CORE-2019-813), and the Foundation for Barnes-Jewish Hospital (3770 and 4642). Electron microscopy and data generation were performed by G. Strout, S. Sviben, and J. Fitzpatrick. Phycoethrin-labeled and allophycocyanin-labeled H2-Kb-SIINFEKL tetramers were obtained through the NIH Tetramer Core Facility. *S. epidermidis* strain NIHLM087 was a gift from J. Segre (NIH). pMS182 (pLI50-Ppen-GFP-mut2) was a gift from S. Walker (Harvard University). B16-FO-OVA was a gift from N. Reticker-Flynn and E. Engleman (Stanford University). **Funding:** M.A.F. was supported by Open Philanthropy, the Howard Hughes Medical Institute (HHMI)–Simons Faculty Scholar Award, the Leona M. and Harry B. Helmsley Charitable Trust, the Chau Hoi Shuen Foundation, NIH grant DK110174, the Chan Zuckerberg Biohub, Stand Up to Cancer, the Stanford Microbiome Therapies Initiative, and MAC3 Impact Philanthropies. Y.E.C. was supported by an HHMI Hanna H. Gray Fellowship. D.B. was supported by an Early Postdoc Mobility Fellowship from the Swiss National Science Foundation. K.N. was supported by the Human Frontier Science Program LT000493/2018-L and a Fellowship of the Astellas Foundation for Research on Metabolic Disorders. Y.B. was supported by the Division of Intramural Research of NIAID (1ZIA-AI001115 and 1ZIA-AI001132). **Author contributions:** Conceptualization: Y.E.C., D.B., K.N., Y.B., and M.A.F. Methodology: Y.E.C., D.B., K.N., Y.B., and M.A.F. Investigation: Y.E.C., D.B., K.A., A.D., A.Z., N.E., V.K.Y., and A.V. Visualization: Y.E.C., D.B., and M.A.F. Funding acquisition: Y.E.C., D.B., K.N., Y.B., and M.A.F. Supervision: Y.E.C., D.B., Y.B., and M.A.F. Writing – original draft: Y.E.C. and M.A.F. Writing – review and editing: Y.E.C., D.B., A.V., Y.B., and M.A.F. **Competing interests:** M.A.F. is a cofounder and director of Federation Bio, a company developing microbiome-based therapeutics. Y.E.C. and K.N. were consultants for Federation Bio. Y.E.C., D.B., K.N., and M.A.F. are inventors on patent applications submitted by Stanford University and the Chan Zuckerberg Biohub that cover methods for using engineered bacteria to elicit antigen-specific immune cells (patent application no. US20220362358). **Data and materials availability:** All data are available in the main text or supplementary materials.

SUPPLEMENTARY MATERIALS

science.org/doi/10.1126/science.abp9563
Materials and Methods
Figs. S1 to S10
Tables S1 and S2
References (*53*–*68*)
MDAR Reproducibility Checklist

View/request a protocol for this paper from *Bio-protocol*.

Submitted 8 March 2022; accepted 28 February 2023
10.1126/science.abp9563